

Research Paper

# Maximum Tension Lines of MSE Embankments with Polymer and Metallic Reinforcements on Different Foundations Types

D.T. Bergado<sup>1</sup>, S. Chaipayut<sup>2\*</sup>, R.M. Basilio<sup>3</sup>, T. Hino<sup>4</sup>, and O. Sukchaisit<sup>5</sup>

## ARTICLE INFORMATION

### Article history:

Received: 8 Maret 2021

Received in revised form: 19 June 2021

Accepted: 10 August 2021

Publish on: 06 December 2021

### Keywords:

Mechanically stabilized earth (MSE)

Reinforced embankment

Maximum tension line

Potential failure plane



This work is licensed under the Creative Commons Attribution International License (CC BY 4.0)

<https://creativecommons.org/licenses/by/4.0/>

## ABSTRACT

Four full scale and fully instrumented mechanically stabilized earth (MSE) test embankments were constructed to 6 m high for analyses and comparison of their behaviour, namely: one on hard ground, one on DCM improved ground and two on soft ground. The MSE on hard ground was reinforced with strong polymer geogrid in one side as well as metallic grids and strips in the other side. The MSE on improved ground was reinforced with hexagonal grids. Due to the negligible vertical and lateral movements in hard and improved ground, the consequent maximum tension lines were observed to closely follow the bilinear Coherent Gravity Method with standard distance from the facing of  $0.3H$  where  $H$  is the equivalent height of the reinforced embankment. Moreover, two fully instrumented MSE were constructed on soft ground having similar trapezoidal cross-sections. One embankment was reinforced with polymer geogrids and the other with steel grids. The resulting large vertical and lateral movements of both embankments have almost identical patterns. The maximum tension lines of both embankments closely resemble to that of Coherent Gravity Method but with location of the vertical line portion at closer distances of  $0.1H$  to  $0.2H$  from the embankment facing.

## 1. Introduction

The concept of reinforcement using tensile members to strengthen the backfill soil has become widely popular

in the practical applications in geotechnical engineering (Li et al., 2014). The introduction of installing steel strips in early 1970s followed by geotextiles and geogrids have approached to the new era of designing reinforced soil

<sup>1</sup> Professor Emeritus, Geotechnical and Earth Resources Engineering, School of Engineering and Technology, Asian Institute of Technology, Pathumthani 12120, Thailand, dbergado@gmail.com

<sup>2</sup> Assistant Professor, Department of Civil Engineering, Faculty of Engineering, King Mongkut's Institute of Technology Ladkrabang, Bangkok 10520, Thailand, salisa.fern@gmail.com, salisa.ch@kmitl.ac.th (\*corresponding author)

<sup>3</sup> Professor, University of Northern Philippines, Vigan City 2700, Philippines, rey26bailio@yahoo.com.ph

<sup>4</sup> Professor, Department of Science and Engineering, Faculty of Science and Engineering, Saga University, Saga 840-8502, Japan, hino@ilt.saga-u.ac.jp

<sup>5</sup> Student, Department of Civil Engineering, Faculty of Engineering, King Mongkut's Institute of Technology Ladkrabang, Bangkok 10520, Thailand, japanjj1@gmail.com

Note: Discussion on this paper is open until March 2022

structures (Voottiprex, 2000; Yang et al., 2010). A mechanically stabilized earth (MSE) or geosynthetic MSE wall has been widely used with a combination of embankment installed with geosynthetic material since 1970s in order to design the stabilized embankment for road, pavement, air-fields, etc. There have been produced several practical guidelines to design the MSE wall which give different results in accordance with the methodologies adopted in that particular projects. The internal and external stabilities of MSE structures depend on the strength of reinforced material, strength of backfill soil, influence of surcharge load and the design and construction methods of MSE embankment (Hossain et al., 2012; Moudabel et al., 2014; Won et al., 2018; Hulagabali1 et al., 2018).

The concept of MSE embankment is to add tensile strength of the backfill soil which is strong in compression. In this approach, the reinforcement consisting of polymer geogrid and steel grids having higher stiffness and tensile strength are installed in the MSE embankment incorporating two significant functions. The first function reduces/restrains the lateral displacement of the MSE wall by mobilizing tensile force in the reinforcement. And the second one applies in the modification of the strain pattern in the reinforced soil mass owing to the influence of the interface shear stresses. Consequently, the MSE embankment can function as composite material strong in both compression and tension.

The inextensible and extensible materials refer to steel grids and polymer geogrids, respectively. To assess the internal stability design of geosynthetic and steel reinforced soil walls, appropriate estimations of soil reinforcement loads and deformations are necessary. The predicted reinforcement loads influence the strength and spacing needed for the reinforcement as well as the reinforcement length to resist pull-out. Current design methodologies use limit equilibrium concepts to calculate reinforcement loads. Two limit equilibrium methods can be used in design specifications to estimate reinforcement loads consisting of: (i) the Tieback Wedge/Simplified Method (AASHTO, 2002), and (ii) the FHWA Structure Stiffness Method or Coherent Gravity Method (Christopher et al., 1990). Generally, the Coherent Gravity Method is utilized to design the MSE embankment with an inextensible reinforcement (Anderson et al., 1987; Anderson et al., 2010). The tension envelope can be described with a bilinear function. While, the Tieback Wedge Method is used to design the MSE embankment with an extensible reinforcement with the maximum tension lines inclined at  $45^\circ + \phi/2$ .

The objectives of this study are twofold, namely: 1) To measure the vertical and lateral movements as well as

the tension forces in the reinforcements of four full scale MSE embankments with metallic and polymer reinforcements constructed on hard, soft and improved foundation and 2) To evaluate and compare the locations of the maximum tension lines in the four full scale test embankments constructed on hard, soft and improved foundation. It is envisaged that the measured tension in the reinforcements are influenced by the vertical and lateral movements of the reinforced full-scale embankments.

## 2. Maximum tensile force analysis method

The maximum tension line divides the MSE embankment into two zones, namely: the active zone and the resistant zone (**Fig. 1**). The active zone and the backfill soil tend to move outward from the MSE embankment. The backfill soil is at the failure condition coinciding with the maximum tension plane or line. The tensile force and the length of reinforced material can increase the friction resistance and increase the stability of the MSE embankment. The interface shear forces from the interaction between the reinforcement and backfill soil in the resistant zone as well as the tension resistance of the reinforcements provide the resistance force against the pullout of the active zone.

The failure plane or line of retained backfill soils have been proposed by Rankine and Coulomb. Rankine's method assumed that there is no friction or adhesion between the soil and the retaining structure **Fig. 2a**) with consequent linear failure surface or line. Coulomb developed a method of determining lateral pressures that

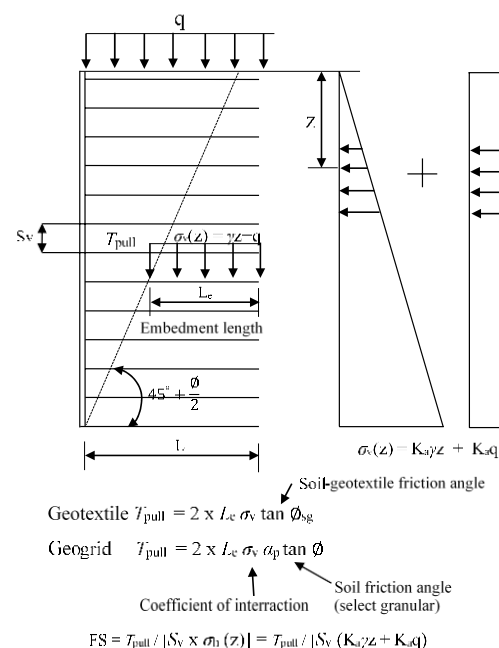


**Figure 1.** Sample calculation of factor of safety (F.O.S) for geotextile reinforcement linear failure plane.



$$T_{max} = S_v K_a [\gamma(z+S)+q] \quad [1]$$

where:

- $S_v$  = tributary area for reinforcement layer equivalent to the vertical spacing of the reinforcements,  
 $K_a$  =  $(1-\sin\phi)/(1+\sin\phi)$  is the coefficient of active earth pressure, determined with a horizontal backslope and no wall-soil interface friction  
 $\gamma$  = unit weight of the soil  
 $Z$  = depth of reinforcement layer below the top of the wall  
 $S$  = equivalent soil height of uniform surcharge pressure  
 $q$  = surcharge pressure.

In the FHWA Structure Stiffness (Coherent Gravity) Method, the earth pressure coefficient,  $K_r$ , is increased by a factor which is dependent on the depth below the wall crest, reinforcement type, and global wall stiffness (Figs. 4 and 6). The maximum load in the reinforcement layer can be:

$$T_{max} = S_v K_r (\gamma[Z+S]+q) \quad [2]$$

$$K_r = K_a (\Omega_1 (1+0.4(S_r/47,880)) (1-(z/6)) + \Omega_2 (z/6)) \text{ if } z \leq 6\text{m}$$

$$K_r = K_a \Omega_2 \text{ if } z > 6\text{m}$$

$$S_r = J/(H/n)$$

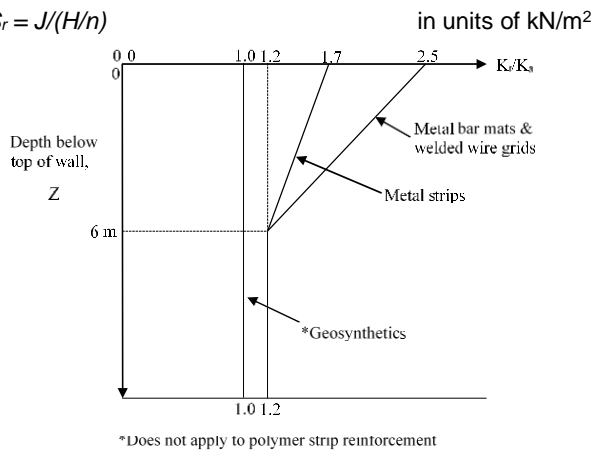


Figure 6. Determination of  $K_r/K_a$  for simplified method [13].



Figure 7. Photographs of test embankments: (a) vertical face with metallic reinforcements and (b) sloping face with polymer reinforcements.

where:

- $K_r$  = lateral earth pressure coefficient  
 $S_r$  = global reinforcement stiffness for the wall  
 $\Omega_1$  = dimensionless coefficient equal to 1.0 for strip and sheet reinforcement or equal to 1.5 for geogrid and welded steel grid.  
 $\Omega_2$  = dimensionless coefficient equal to 1.0 if  $S_r \leq 47,880$  kPa or  $\Omega_2 = \Omega_1$  if  $S_r > 47,880$  kPa.  
 $J$  = average reinforcement stiffness for the wall (in units of force per running unit length of wall)  
 $H/n$  = average vertical spacing of the reinforcement ( $H$  is the height of the wall and  $n$  is the total number of reinforcement layers)

The ratio of  $K_r/K_a$  is shown in Fig. 6 corresponding to the different types of extensible and inextensible reinforcements (Allen et al., 2004).

#### 4. The full-scale test embankment on hard ground in Phitsanulok province, Thailand

A full-scale reinforced earth embankment was designed and constructed by Thailand Department of Highways (DOH) (Nuakliang, 2011; Duangkhae, 2013; Duangkhae et al., 2013; Shrestha et al., 2014). The site of construction is near the Highway No.11 Phitsanulok-Uttaradit at KM No. 12. There were two types of reinforcements. One side was reinforced with polymer grids and had a steep slope of 70 degrees from the horizontal with soil bags facing called reinforced soil slope (RSS) (Figs. 7b and 8). The other consisted of mechanically stabilized earth wall (MSEW) with concrete panel facing (Figs. 7a and 8). The RSS and MSEW test embankment were designed to 6 m of height, 15 m of width and 18 m of length. On the side of reinforced soil slope (RSS) three different types of polymeric geogrids reinforcement were installed, namely: polypropylene (PP), high density polyethylene (HDPE) and polyester (PET) (Fig. 9). At the other side, the mechanically stabilized earth wall (MSEW) was constructed with two types of metallic reinforcements such as metallic strip (MS) and steel wire grid (SWG) (Fig. 9). The vertical spacing between each reinforcement layer was 0.5 m and the length was 5 m (upper layers of metallic strip from layer 7 to layer 12 have 5.80 m length). Comparison on the behaviour of the two reinforcing materials such as polyester (PET) and steel wire grid (SWG) were made. The backfill materials consist of silty sand mixed with lateritic soil at 50%:50% by volume. The soil profile showing hard foundation is given in Fig. 10. The hard foundation consists of interlayering of dense to very dense sand and very stiff to hard clay. The standard

**Table 1.** Material properties of reinforced embankment on hard foundation [16-17].

Material Name	Tensile Strength (kN/m)	Thickness (mm)	Normal Stiffness, EA (kN/m)
Metallic Strip (MS)	277.6	4.00	88,000
Steel Wire Grid (SWG)	128.1	6.00	35,000
Polyester (PET)	83.6	1.50	925
Polypropylene (PP)	91.9	1.45	1,360
High-Density Polyethylene (HDPE)	85.8	1.91	1,320

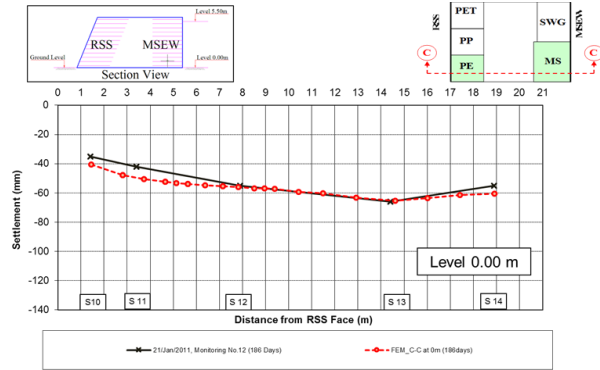


**Figure 8.** Section and plan views of test embankment with measured and simulated vertical settlements at PE-MS section [24].

monitoring instruments consisted of inclinometers, strain gauges, piezometers, plate settlements and pressure cells. The strain gages in the metallic reinforcements consist of vibrating wire strain gages while fiber optic was utilized in the polymer reinforcements. The material properties of the components of the reinforced embankment on hard ground are tabulated in **Table 1**. The photographs of the vertical face of the metallic reinforcements and sloping face of the polymer grid reinforcements are shown in **Figs. 7a and b**, respectively.

**5. Hexagonal grid reinforced test embankment on soft Bangkok clay improved with deep cement mixing (DCM)**

**5.1 Test location and subsoil profile**

The test location of the field test embankment is located at Wangnoi Power Plant Site which is located within the Central Plain of Thailand (Lai et al., 2006). The plan layout and cross-section the test embankment are shown in **Fig. 11 a, b, c** with dimensions of 19 m long and 6 m wide. The 6 m high vertical embankment facing consisted of patented precast concrete panels with 150mm thickness and surface area of 2.25 sq. m. (**Fig. 12a**). The concrete strength of each panel was 30 MPa.

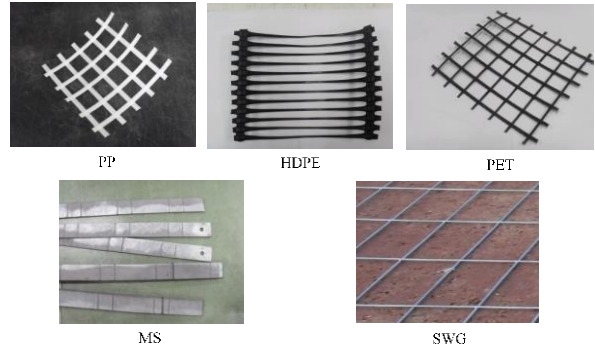


**Figure 9.** Photographs of polymer and metallic reinforcements.

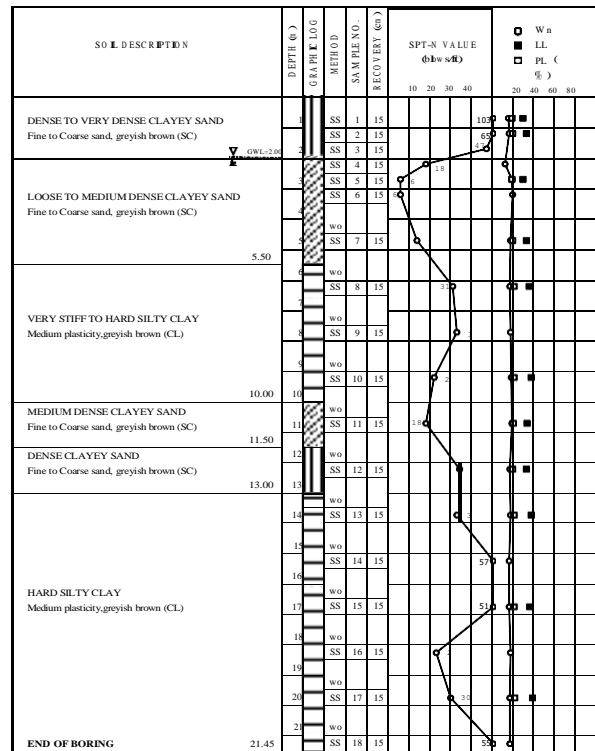


**Figure 10.** Soil profiles at hard foundation site [15].

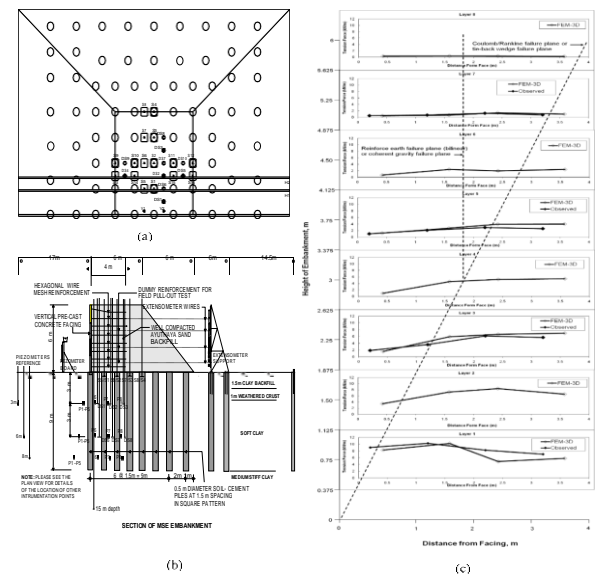


**Figure 11.** Plane and cross-section of hexagonal grid reinforced embankment on soft Bangkok clay improved with deep cement mixing (DCM) piles with measured and FEM simulated tensile forces in the reinforcements.

The embankment was made of well-compacted silty-sand backfill reinforced with 1.0 m wide x 5.0 m long PVC-coated hexagonal wire grid at 0.75 m vertical spacing (**Fig. 11b**). The backfill soil has compacted unit weight of 18.20 kN/m<sup>3</sup>, cohesion of 7.70 kPa and angle of internal friction of 22 degrees, and it has maximum dry density and optimum water content of 16.1 kN/m<sup>3</sup> and 15%, respectively. Strain gages were installed at designated locations of the selected hexagonal wire grid reinforcements.

The site was underlain by the well-known soft Bangkok clay. The properties of soft clay foundation at the Wangnoi site are indicated in **Fig. 13b** which are similar the soil profile at AIT Campus in **Fig. 13a**. The Wangnoi site is located approximately 30 KM from AIT Campus. The soft clay, which is overlain by 1.0 m thick weathered crust and 1.5 m thick clay backfill, was encountered from 2.5 m to 9.0 m depth. The undrained shear strength obtained from field vane test of the soft clay was less than 15 kPa. Underlying the soft clay layer is medium to stiff clay layer, having undrained shear strength of more than 50 kPa.

5.2 Monitoring instrumentations

The embankment and the improved foundation were instrumented. Piezometers (P), which monitored the dissipation of excess pore water pressures in the foundation soils during and after deep mixing (jet grouting), were installed at various points underground within and outside the embankment zone. Surface

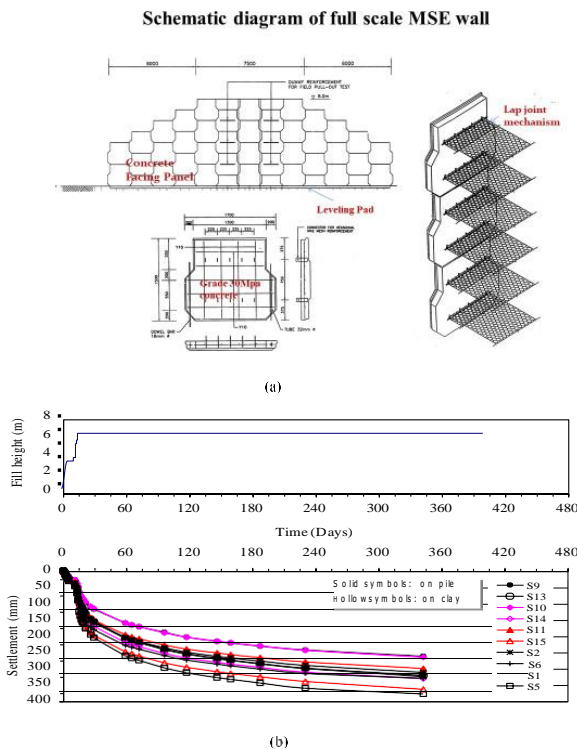


**Figure 12.** Front view and settlement with time of hexagonal grid reinforced embankment on soft Bangkok clay improved with deep cement mixing (DCM) piles.

settlement plates (S) were installed both “on pile” and “on clay” at the bottom of embankment. Deep settlement plates (DS) were also installed at 3.0 m and 6.0 m depths at few locations as shown in **Fig. 11a**. In addition, vertical (V) and horizontal (H) inclinometers were placed near the vertical side of the embankment to measure the lateral displacement and settlement profile, respectively.

6. The full scale MSE test embankment on soft Bangkok clay

6.1 Test location and subsoil profile

The full scale MSE wall test was constructed on a soft Bangkok clay at the Asian Institute of Technology (AIT), Thailand. **Figure 13a** illustrates the subsoil profile at the construction site consists of topmost 2.0 m thick layer of yellowish-brown weathered clay overlying a blackish-gray soft clay layer, which extends up to a depth of about 8.0 m below the existing ground. The soft clay layer is underlain by a stiff clay layer. The ground water table fluctuates in between 1.0 to 2.0 m below the ground surface.

6.2 Polymer geogrid reinforced MSE test embankment on soft Bangkok clay

The MSE embankment with an extensible reinforcement was constructed with Tenax polymer geogrid reinforcement on soft Bangkok clay at the campus of the Asian Institute of Technology, Bangkok, Thailand. The polymer geogrid is made up of uniaxially

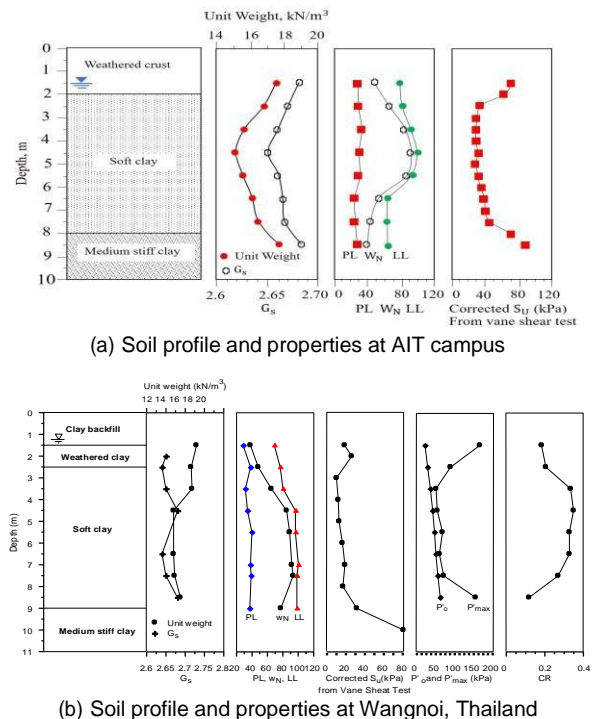


**Figure 13.** Soil profile and properties of soft Bangkok clay in the central plain of Thailand.

**Table 2.** The physical properties of polymer geogrid reinforced MSE wall [19-20].

Physical characteristics	Data		
Structure	Mono-oriented geogrid		
Mesh type	Oval apertures		
Standard colour	Black		
Polymer type	HDPE		
Packaging	Rolls in polyethylene bags with label		

Dimensional characteristics	Polymer geogrid	Unit	Notes
Aperture size MD	120/140	mm	b,d
Aperture size TD	13/17	mm	b,d
Product unit weight	450	a/ma	b
Roll width	1.0	m	b
Roll length	40	m	b
Roll diameter	0.28	m	b
Roll volume	0.072	mc	b
Gross roll weight	18.5	kg	b

Technical characteristics	Polymer geogrid	Unit	Test method	Notes
Peak tensile strength	45.0	kN/m	GRI-GGI	a,c
Yield point elongation	12.0	%	GRI-GGI	b,c
Tensile strength at 2% strain	13.0	kN/m	GRI-GGI	a,c
Tensile strength at 5% strain	26.0	kN/m	GRI-GGI	a,c
Characteristics strength	16.4	kN/m	GRI-GGI	b,e

**NOTES:**

- 95% lower confidence limit values
- Typical values
- Tests performed using extensometers at 50 mm/min speed
- MD : machine direction (longitudinal to the roll)  
TD : Transversal direction (across roll width)
- Test performed at 20° C

oriented high-density polyethylene to receive higher tensile strength. The polymer geogrid has a maximum tensile strength of 55 kN/m. The physical properties of polymer geogrid and its characteristics are shown in **Table 2**.

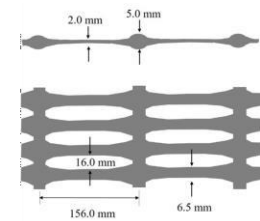
The instrumented MSE wall has a total height of 6.0 m with 5.7 m above the existing ground surface and 0.3 m excavated below the natural ground surface. It has a vertical face in front and a sloping face of 1:1 at the back. The MSE wall face has consisted of vitcomats placed inside the wrapped portion of the geogrid to prevent erosion of the soil (**Fig. 14a**).

The weathered clay backfill was spread over the geogrid and compacted at equal interval of 0.15 m thickness to confirm efficient and well compaction. The vertical spacing between the reinforcing grids were 0.30 m and 0.6 m for the lower 9 layers and the upper 9 layers, respectively.

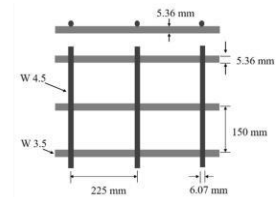
Each layer was compacted with the combination of hand compactor and vibratory roller to obtain the density of about 95% of the standard Proctor density, with the placement moisture content varying at  $\pm 1\%$ ,

**Table 3.** The properties of welded wire mesh reinforced MSE wall from the previous studied [21-22].

Properties	Fill material type		
	Clayey sand	Lateritic soil	Weathered clay
Peak triaxial friction angle, $\phi'_{tx}$ : °	24	25.2	24
Cohesion, $C'$ : kN/m <sup>2</sup>	10	20	30
Unit weight of the soil, $\gamma$ : kN/m <sup>3</sup>	17	19.3	16.3
Height of the wall, $H$ : m	5.7	5.7	5.7
Equivalent height of uniform surcharge pressure, $S$ : m	0	0	0
Tributary area, $S_v$ : m	0.45	0.45	0.45
Tensile stiffness, $J_1 = J_2$ : kN/m	36000	36000	36000



(a) Geogrid embankment with Tenax TT201 SAMP polymer grid reinforcements



(b) Steel grid embankment with galvanized welded wire steel grids reinforcements

**Figure 14.** Geogrid and steel grid reinforced test embankments at AIT Campus, Bangkok, Thailand.

corresponding to that optimum moisture content determined by standard Proctor test. The overall construction of the MSE wall had completed in 38 days. In order to observe the behaviour of the full scale MSE embankment, monitoring instruments consisting of pneumatic piezometers, hydraulic piezometers, fill settlement plates, surface settlement plates, subsurface settlement plates, earth pressure cells and an inclinometer were installed (**Fig. 15**). The observed data were derived from the research works of Menil (1993) and Basilio (1994).

### 6.3 Steel grid reinforced MSE test embankment on soft Bangkok clay

The full scale steel grid reinforced MSE embankment was also constructed on soft Bangkok clay at the campus of the Asian Institute of Technology (AIT), Thailand by the research works of Shivashankar (1991) and Bergado et al. (1991a; 1991b). The subsoil profile (**Fig. 8a**) of the

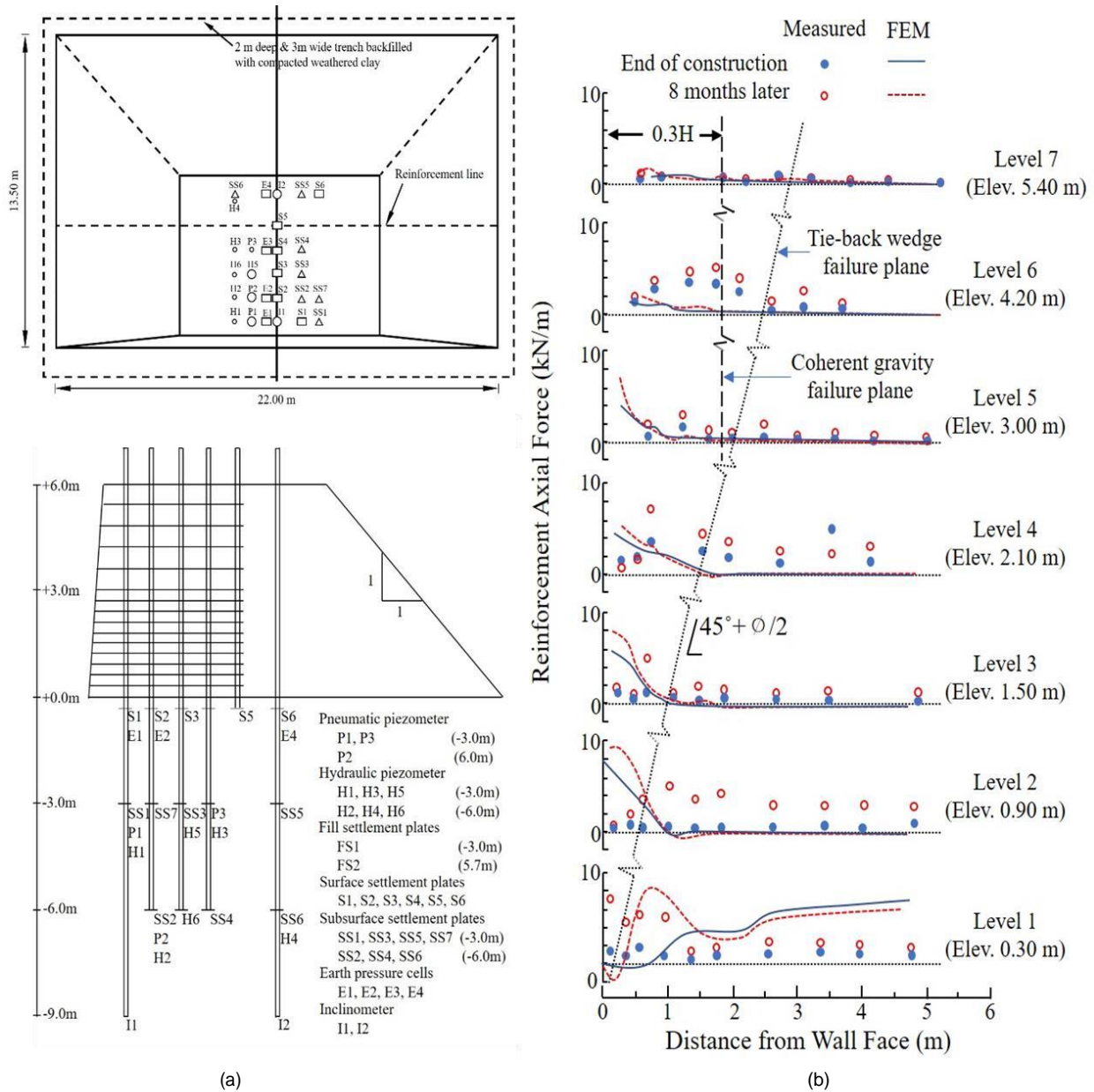


**Figure 15.** Plan and cross-section of geogrid reinforced embankment with measured and simulated tensile forces in the reinforcements: (a) plan and cross-section of geogrid embankment indicating reinforcement instrumentations (b) measured and simulated reinforcement tensile forces at geogrid embankment.

MSE wall foundation consisted the uppermost 2.0 m thick weathered clay layer underlain by a 6.0 m thick soft clay layer and followed by a 6.0 m thick stiff clay layer. The steel grid reinforced MSE embankment (Fig. 14b) was constructed with 5.70 m height, 14.64 m length (at the top of MSE wall) and 26.04 m length (at the bottom of MSE wall), that has similar dimensions with that of the geogrid full scale MSE wall test. This MSE test embankment was divided into three sections of embankment fills, namely: clayey sand (CS), lateritic soil (LS) and weathered clay (WC) along its length. The properties of backfill soil are tabulated in Table 3 together with the properties of the steel grid reinforcements.

The reinforced material was characterized with welded

wire mesh, which is 2.44 m wide and 5.0 m long and consisted of 6.07 mm x 5.36 mm diameter size bars with 0.15 m x 0.225 m grid openings. The welded wire meshes were installed with vertical spacings of 0.45 m. The behaviour of welded wire mesh MSE wall was measured by seven mats instrumented with self-temperature compensating electrical resistant strain gauges for each section as shown in Fig. 16.

## 7. Results and Discussions

### 7.1 Metallic and polymer grid reinforced MSE embankment of hard ground

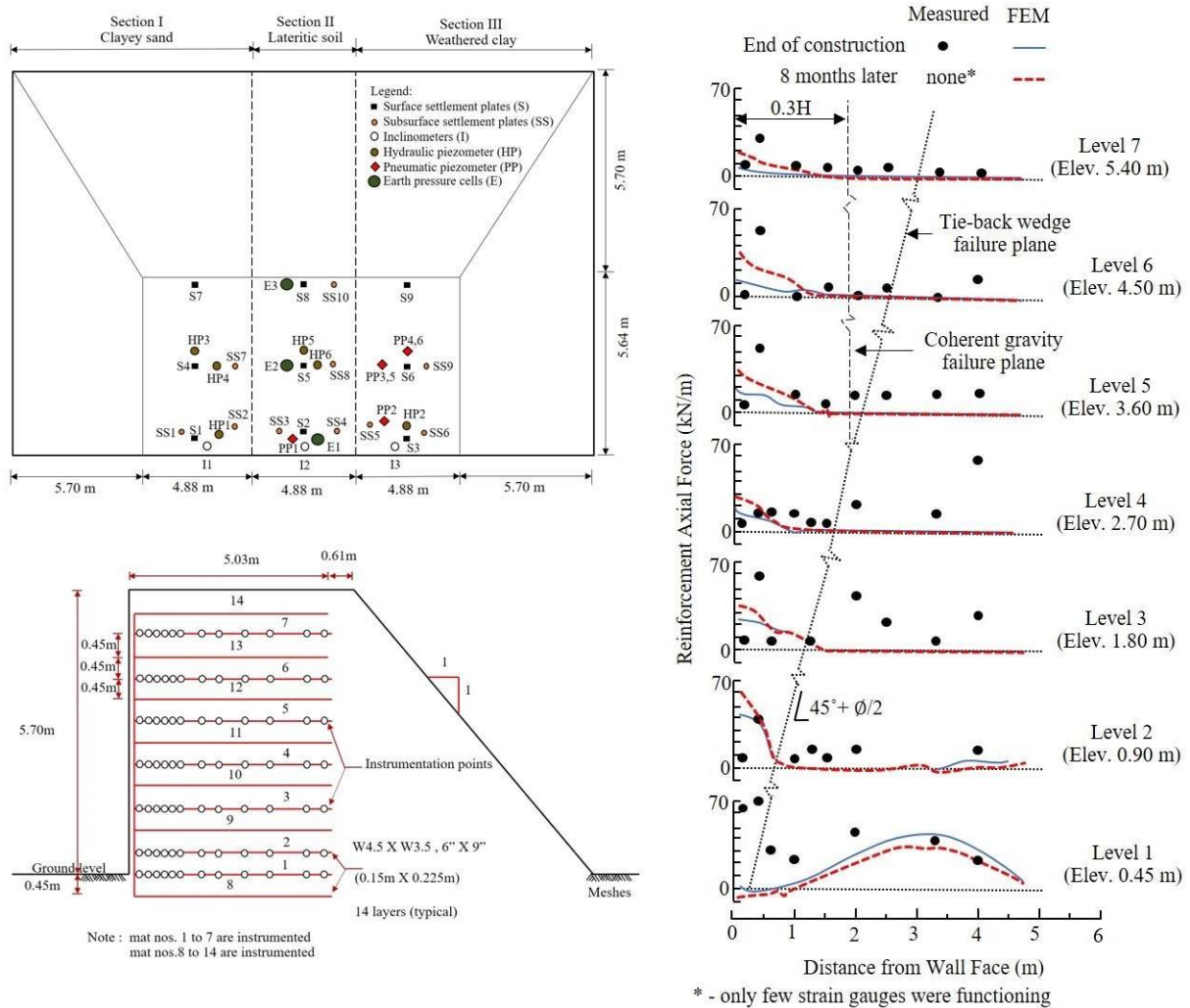


**Figure 16.** Plan and cross-section of steel grid reinforced embankment with measured and simulated tensile forces in the reinforcements.

The vertical settlements, lateral movements and reinforcement strains are plotted in **Figs. 8, 17, 18, and 19** together with the FEM simulations by Baral, (2013) and Baral et al. (2016). As expected with reinforced embankment on hard foundation, the vertical settlement at PE-MS section were very small ranging from 40 to 60 mm as indicated in **Fig. 8**. The settlements of the embankment and its foundation were very low because the embankment was constructed on hard ground. The corresponding lateral deformations obtained from the inclinometers were equally negligible as given in **Fig. 17 a, b**. However, additional lateral movement occurred near the top of the RSS embankment when an unreinforced 1.2 m thick backfill was added after completion of construction. The measured strains in the reinforcements for the polymer geogrids and the metallic grids are shown in **Figs. 18 and 19**, respectively. According to the standard behaviour, the maximum strains in the stiff polymeric reinforcements

seemed to follow the bilinear Coherent Gravity Method (**Fig. 4**) since the strengths of the geogrid reinforcements were high as tabulated in **Table 1**. Furthermore, the corresponding maximum strains in the metallic reinforcements tended to follow the bilinear Coherent Gravity Method (**Fig. 4**).

**7.2 Hexagonal grid MSE embankment on soft Bangkok clay improved with deep cement mixing (DCM) piles**

**7.2.1 Surface settlement**

**Figure 12b** shows the observed surface settlements from all installed surface settlement plates at the base of the test embankment. At 397 days after the end of construction, the average surface settlements as measured from all the settlement plates on ground and on piles are 327.54 mm and 277.76 mm, respectively. The average subsurface settlement at depths of 3.0 m and 6.0 m were 243.97 mm and 71.44 mm, respectively.

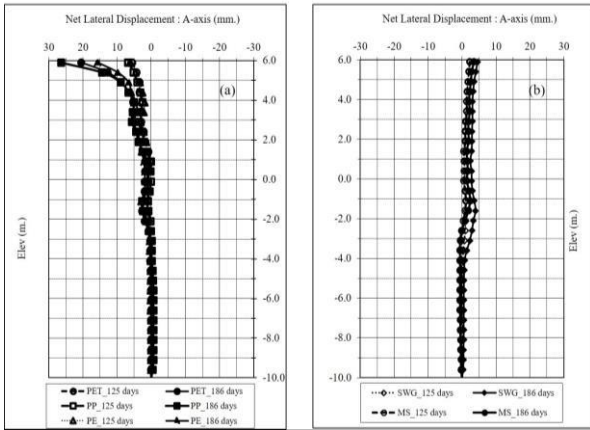


Figure 17. Lateral deformations obtained from inclinometers: a) Polymer and b) Metallic reinforcements [15].

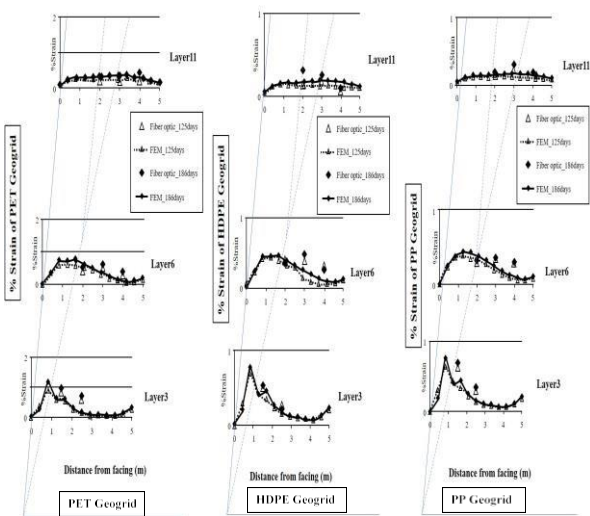


Figure 18. Measured strains at different levels of PET, HDPE and PP geogrid polymer reinforcements [15].

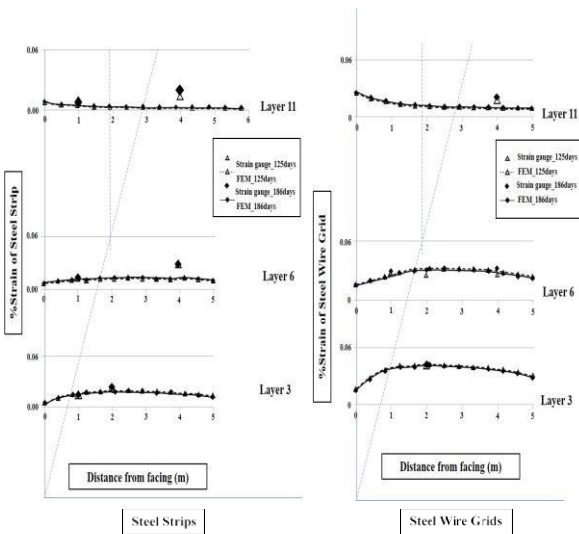


Figure 19. Measured strains at different levels of steel strip and steel wire grid reinforcements [15].

7.2.2 Comparison of vertical settlements and lateral deformations of test embankment with and without deep cement mixing (DCM) piles

In order to investigate the effects of vertical and lateral deformations of test embankments on the tensile forces in the reinforcements, comparisons were made as shown in Fig. 20a, b. The vertical and lateral deformations of steel grid reinforced embankment on soft Bangkok clay were compared to the corresponding values of hexagonal grid reinforced embankment on soft Bangkok clay improved with deep cement mixing (DCM) piles. The total vertical deformations were reduced by as much as 60% and the total lateral movement were reduced by as much as 75%. Similar behaviour were studied by Edincliiler and Guler (1995) using lime stabilized soft clay foundation.

7.2.3 Measured tensile forces in the hexagonal grid reinforcements

There were eight layers of reinforcement installed in the test embankment, namely: layer 1 to 8 where layer 1 being at the lowest elevation at 0.375 m and layer 8 being at the highest elevation at 5.625m from the ground surface. Consequently, layer 1 was having maximum overburden pressures from the backfill soil while layer 8 was having the lowest. The simulated results show that the tension force was maximum at layer 1 and minimum at layer 8 as expected. Figure 11c shows that observed data was more or less in agreement with simulated results at layer 1, 3, 5 and 7 with some signs of overestimations at locations near the wall face and underestimations at locations away from the wall face. This is due to the limitations of the simulation during the consolidation process (Lai et al., 2006). The maximum tension line generally agreed well with coherent gravity bilinear failure plane. Thus, the improved soft ground using deep cement mixing (DCM) functioned similar to the hard ground in Section 7.1 with similar tendencies in the measured tensile forces in the reinforcements of the overlying MSE structure.

7.3 Polymer geogrid MSE embankment on soft Bangkok clay

The monitoring of the full scale MSE wall with polymer geogrid were comprised of settlement, lateral displacement, vertical earth pressure (at the base of the MSE wall), and geogrid strain measurements. The measured data were used to evaluate the applicability of the selected design guidelines in soft Bangkok clay.

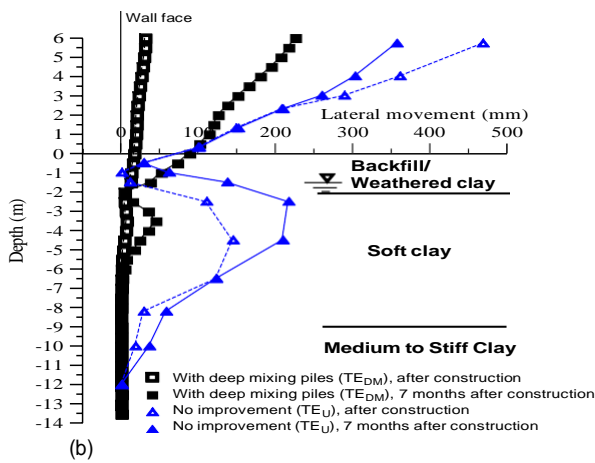
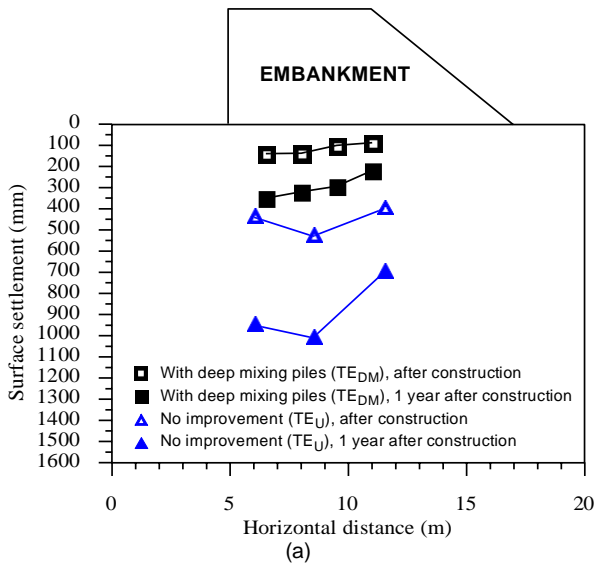


Figure 20. Comparison of vertical and lateral deformations of steel grid reinforced test embankment on soft Bangkok clay and hexagonal grid reinforced embankment on soft Bangkok clay improved with deep cement mixing (DCM) piles.

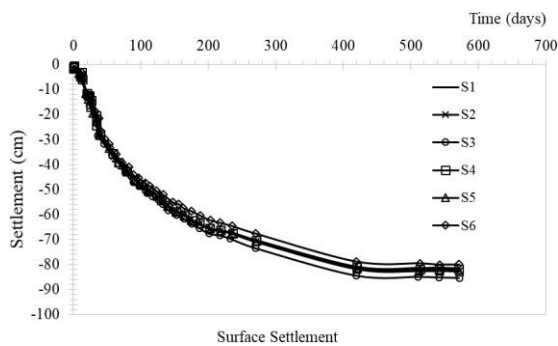


Figure 21. Observed surface settlement of polymer geogrid reinforced embankment [19]

7.3.1 Settlements

A classical behaviour of surface settlements on soft ground construction were continuously followed in the site as reflected by the settlement curves in Fig. 21. It started with an initially high rate of settlement during construction, slowing down for some time reaching a point beyond which the rate of settlement seems to be constant. About 200 days after the end of construction,

the rate of settlement decreased considerably. After 400 days, the rate of settlement is so small that the curves appeared flat. The settlement data confirmed that 90% of consolidation started before 400 days after the end of construction.

The surface settlements indicated by S<sub>1</sub> to S<sub>6</sub> were observed to be nearly identical. Figure 21 showed that at the end of 570 days, the magnitude of surface settlements in all locations did not differ much from each other. The last monitored reading showed maximum values at S<sub>3</sub> and S<sub>4</sub>, both located at the centre of the MSE embankment at 0.85 m. From Fig. 21, the magnitude of settlement tended to increase towards the centre of the structure. These patterns of settlement surface signified that much of the vertical pressure are situated at the centre of the MSE embankment.

7.3.2 Lateral displacement

The horizontal movements, both in the MSE wall (at the face and at the back of the MSE wall) and the subsoil, were monitored by a biaxial inclinometer. Figure 22 reflects the lateral displacements along with time at post construction phase during the first and second stages of monitoring near the MSE wall face. At the first stage of monitoring (referring 7 days up to 223 days) the lateral ground movements in the foundation occurred mainly at 3.0 m to 4.0 m depth toward the outward direction. The movements at the base were very minimal with the maximum lateral movement occurring at the top of the MSE wall test. At this point, it was apparent that the rotation of the MSE wall was encountered around the toe. This trend was continuously observed at the second stage of the observation (referring 420 days up to 570 days) with the maximum outward movement recorded at the top of the MSE wall.

7.3.3 Maximum tension line

The tension forces of the geogrid reinforcements at different elevations are plotted in Fig. 23 together with

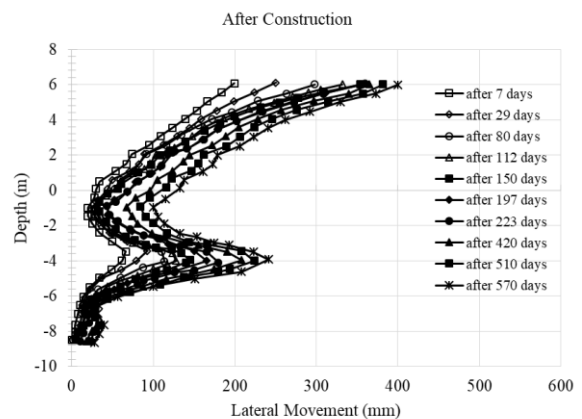
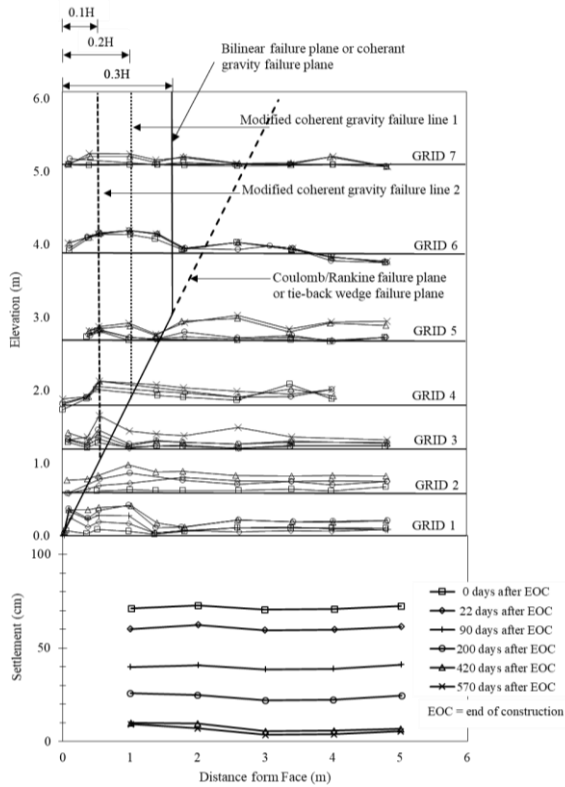
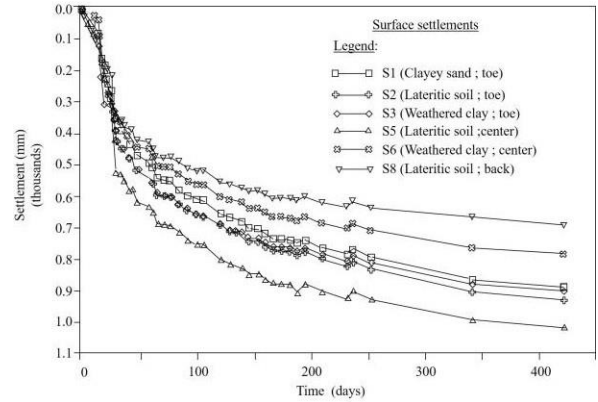


Figure 22. Lateral movement at face of polymer geogrid embankment after construction [19].



**Figure 23.** Proposed maximum tension line polymer geogrid reinforced embankment on soft ground.

the settlements below the test embankment. As presented in the previous sections on hard ground foundation as well as DCM improved foundation, the maximum strains or maximum tension line normally follow either the linear Tieback Wedge Method (Fig. 5) or the Coherent Gravity Bilinear Method (Fig. 4) with distance of  $0.3H$  from the MSE wall face. Previous researches on MSE embankment supported on hard foundation indicated that the maximum tension line can either be defined as linear failure plane described by Rankine type for extensible reinforcements or a bilinear failure plane for high stiffness or inextensible reinforcements. As shown in Fig. 23, the potential failure surfaces for MSE on soft ground did not agree with the above-mentioned failure surfaces on hard foundation. Rather the measured maximum tension line seemed to follow the bilinear coherent gravity method but with the vertical portion at closer distances of  $0.2H$  or  $0.1H$  to the MSE wall face. Moreover, the reinforcements near the base or bottom portion of the MSE also indicated larger tensile forces. These tendencies are due to the effects of large vertical and lateral deformations of the soft ground foundation. Similar behaviour were obtained by Bergado et al. (1995) using numerical simulations for MSE on soft ground with induced large deformations near the facing and bottom of MSE. Duangkhay et al (2013) also observed the increased reinforcement loads due to the large vertical and lateral deformations for MSE on soft



**Figure 24.** Observed surface settlement of steel grid reinforced embankment [20].

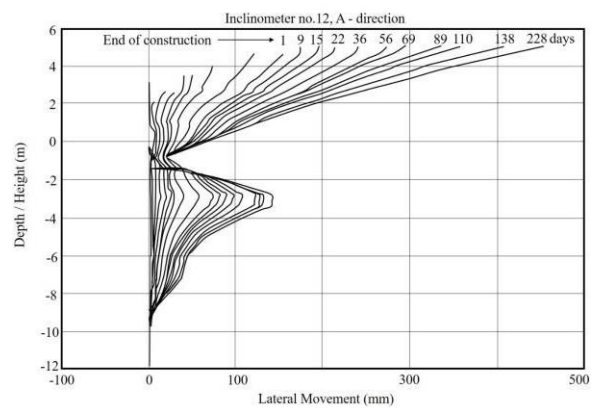


**Figure 25.** Lateral movement at face of steel grid reinforced embankment after construction [20].

ground. Edinçliler and Guler (1995) found that the tensile load in the reinforced material decreases as the strength of foundation increases.

On the basis from the performance of the full scale MSE embankment test reinforced with polymer geogrid, the assumption of a linear failure surface does not work well for MSE on soft Bangkok clay. It is therefore recommended that for polymer geogrid MSE wall on soft ground, the design guidelines using the bilinear failure surface should be adopted.

#### 7.4 Steel grid reinforced MSE embankment on soft Bangkok clay

The previous studies have only incorporated with the welded wire mesh MSE embankment test to focus on the maximum tension line to determine the validity of the assumed failure surface used in the design guideline. The measured surface settlements and lateral deformations are indicated in Figs. 24 and 25, respectively, which are similar to the corresponding values obtained from the geogrid reinforced embankment. The maximum surface settlement was measured as 1.0 m.

##### 7.4.1 Maximum tension line

The tension of reinforced material was immediately measured after construction of the embankment. The monitored data on reinforcement tensions of clean sand (CS), lateritic soil (LS) and weathered clay (WC) backfills were similar. **Figure 26** illustrates the tension of reinforced material measured in weathered clay (WC) backfill together with the settlement profiles plotted at the bottom. The tension distributions in the welded wire mesh MSE embankment for different periods at different elevations were similar to the aforementioned polymer geogrid MSE embankment. The line of maximum tensions did not comply with the potential failure surface defined by either the Rankine type of linear failure plane or the bilinear of Coulomb type with reinforcement failure plane. It was generally observed that the measured maximum tension line agreed with the bilinear failure plane (**Fig. 2c**) of Coherent Gravity Method (**Fig. 4**).

Furthermore, it is noticeable that the assumption of a single failure plane for steel grid reinforced material recommended by Mitchell and Villet (1987) cannot be applied to analyse the behaviour of MSE wall on soft ground. In this reference along with the above-mentioned comparative results, the design guidelines using the bilinear failure surface analysis seems to be more appropriate for MSE embankment on soft ground.

### 7.5 Effect of soft foundation on MSE embankments

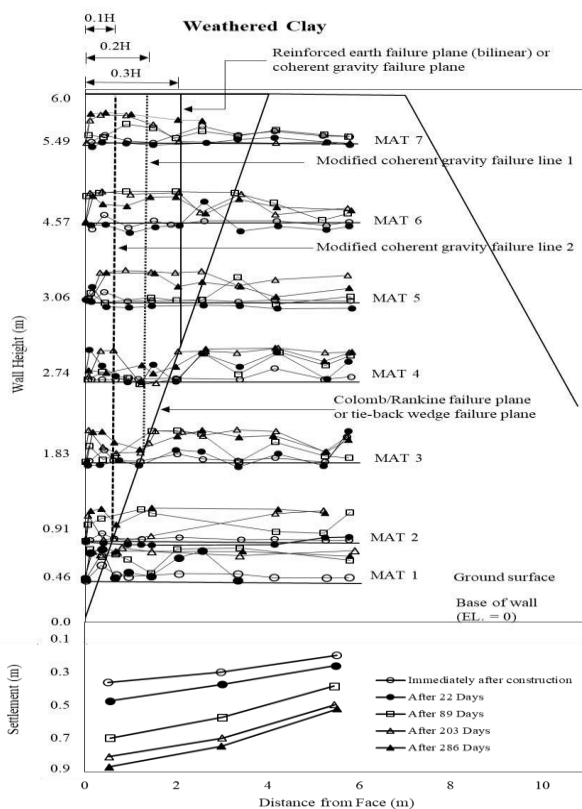


**Figure 26.** Proposed maximum tension line of steel grid reinforcement embankment on soft foundation.

For reinforced embankment on soft ground, the ground/reinforced mass interaction significantly influenced the development of strains in the reinforcements (Bergado et al., 1995; Duangkhae et al., 2013). In this instance, the structural loading can induce the differential ground settlement. The total and differential settlement of the soft clay foundation may cause additional bending and tension loading in the reinforcements of the reinforced soil mass. Consequently, tension loading can occur near the facing and at the bottom of reinforcements and large reinforcement tensile forces occurred nearer to the facing and at the bottom of the reinforced embankment. Both the two full scale MSE embankments with polymer and steel grid reinforcements revealed the aforementioned behaviours together with the occurrences of maximum tensions near the facing as indicated in **Figs. 23 and 26**, respectively. These additional reinforcement tensions of MSE embankment on soft ground were also indicated in a previous study (Duangkhae et al., 2013) where an additional settlement factor was proposed in the K-Stiffness method for reinforced embankment on soft ground.

Additional overburden pressure and lateral stresses have been induced during compaction of the embankment fill. Once the compaction stresses were removed, the additional overburden pressure was also released. However, the lateral stresses were only partially reduced. Some portions remained as "locked in" residual lateral stresses, resulting in the increase of the coefficient of lateral earth pressure, which affected the tensile forces in the reinforcements (Bergado et al., 1991a; 1991b). The compaction effect was significant in the upper reinforcement layers. This compaction effect combined with the bending and tilting of the MSE embankment due to differential settlement may have influenced the shifting of the maximum tension line towards the MSE embankment face in the full-scale tests reinforced with polymer geogrids and steel grids as illustrated by **Figs. 23 and 26**, respectively.

### 7.6 Proposed maximum tension lines for embankments on soft ground

The Coherent Gravity Method as illustrated in **Figs. 3 and 4** is principally used for metallic or inextensible as well as stiff and strong polymer grid reinforcements. The high stiffness of the reinforcement compared to the soil resulting in reduction in the lateral extension in the soil due to the rotation of the principal strain directions (**Fig. 2c**). As a consequence, the lateral earth pressures show larger values than those corresponding to fully active conditions which are consistent during observation.

In this study, the Coherent Gravity Method was not only observed for the MSE embankment reinforced with steel grids but was also exhibited by the MSE embankment reinforced with stiff polymer geogrid. Hence, it is recommended that the design guidelines using the Coherent Gravity Method can be applied for MSE on soft Bangkok clay both for inextensible and stiff extensible reinforcements as shown in **Figs. 23 and 26**, respectively. The standard distance of the maximum tension line from the facing for reinforced embankment on hard ground using Coherent Gravity Method is 0.3H. Due to the occurrence total and differential vertical as well as lateral deformations of reinforced embankments on soft ground, the measured maximum tensile stresses were located nearer to the facing (Bergado et al., 1995; Duangkhae et al., 2013). Thus, the proposed maximum tension line is located at 0.1H to 0.2 H distance from the facing.

## 8. Conclusions

The behaviours of 4 full scale and fully instrumented MSE embankments reinforced with polymer geogrid, hexagonal grids and metallic grids were constructed, one on hard ground, one on DCM improved soft ground and two on soft ground, were compared and analysed with regards to their maximum tension lines. The following conclusions can be made:

- (1) The test embankment on hard ground was reinforced with strong polymer geogrids in one side as well as metallic grids and strip in the other side was constructed to 6 m high.
- (2) Similar hexagonal grid reinforced MSE embankment on DCM improved ground behaved similar to the MSE on hard ground.
- (3) For the embankment on hard ground having negligible vertical and lateral movements with stiff polymer and metallic reinforcements as well as the MSE embankment on improved ground, the maximum tension lines closely followed the bilinear Coherent Gravity Method with the vertical portion at standard distance of 0.3H from the facing.
- (4) Two full scale MSE reinforced test embankments, one reinforced with polymer grid and the other with steel grid, were constructed to 6 m high on soft ground. Subsequently, the tensile loads in the reinforcements were affected by the large vertical and lateral deformations.
- (5) Due to the interaction of MSE embankment on soft ground with the large vertical and lateral deformations, the observed maximum tension line resulted in a modified Coherent Gravity Method with distances varying from 0.1H to 0.2H from the

embankment facing.

## Acknowledgements

This work was supported by King Mongkut's Institute of Technology Ladkrabang (KREF016321).

## References

- AASHTO (American Association of State Highway and Transportation Officials), 2002. Standard specifications for highway bridges, 17 ed. AASHTO, Washington, DC, USA.
- Anderson, P.L., Gladstone, R.A., and Withiam, J.L., 2010. Coherent gravity: the correct design method for steel-reinforced MSE walls. Proceedings of ER2010 Earth Retention Conference 3, ASCE, Bellevue, Washington.
- Baral, P., 2012. Simulations and back-analyses of design parameters of MSE embankment on hard foundation using PLAXIS 3D Software. M. Eng. Thesis No. GT-11-04, Asian Institute of Technology, Bangkok, Thailand.
- Baral, P., Bergado, D.T., and Duangkhae, S., 2016. The use of polymeric and metallic geogrids on a full scale MSE wall/embankment on hard ground: a comparison of field data with simulation. *International Journal of Geo-Engineering*. <https://doi.org/10.1186/s40703-016-0035-6>.
- Basilio, R.M., 1995. Design guidelines for grid reinforced wall/embankment on soft Bangkok clay based on full scale test. M. Eng. Thesis No. GT-94-01, Asian Institute of Technology, Bangkok, Thailand.
- Bergado, D.T., Sampaco, C.L., Shivashankar, R., Alfaro, M.C., Anderson, L.R., and Balasubramaniam, A.S., 1991a. Performance of welded wire wall with poor quality backfills on soft clay. Proc. ASCE Geotechnical Engineering Congress, Boulder, Colorado, USA, : 909-922.
- Bergado, D.T., Shivashankar, R., Sampaco, C.L., Alfaro, M.C., and Anderson, L.R., 1991b. Behavior of welded-wire wall with poor quality cohesive-frictional backfills on soft Bangkok clay: a case study. *Canadian Geotechnical Journal*, **28** (6): 860-880. <https://doi.org/10.1139/t91-103>.
- Bergado, D.T., Chai, J.C., and Anderson, L.R., 1994. Some comments on reinforced earth design, Proc. Conf. on Deep Foundation and Ground Improvement, AIT, Bangkok, Thailand.
- Bergado, D.T., Chai, J., and Miura, N., 1995. FE analysis of grid reinforced embankment system on soft Bangkok clay. *Computers and Geotechnics*, **17**: 447-471.
- Christopher, B.R., Gill, A., and Giroud, S.P., 1990. Reinforced soil structure (I), design and construction guidelines. FHWA RD-89-043, Washington DC, USA.

- Duangkhae, S., 2013. Laboratory and field behavior of reinforced wall/embankment using various reinforcements and facing systems. D.Eng Dissertation No. GT-12-03, Asian Institute of Technology, Bangkok, Thailand.
- Duangkhae, S., Bergado, D.T., Baral, P., and Ocaj, B.T., 2013. Analysis of reinforced embankment on soft and hard foundation. *Ground Improvement Journal*, **66** (G11): 3-23. <https://doi.org/10.1680/grim.13.0000>
- Edincliler, A, and Guler, E., 1999. Geotextile-reinforced embankments on soft clays-effects of a foundation soil crust strengthened by lime diffusion. *Geosynthetics International*, **6** (2): 71-91.
- Hossain, M.S., Kibria, G., Khan, M.S., Hossain, J., and Taufiq, T., 2012. Effects of backfill soil on excessive movement of MSE wall. *J. Perform. Constr. Facil.*, **26** (6): 793-802. [https://doi.org/10.1061/\(ASCE\)CF.1943-5509.0000281](https://doi.org/10.1061/(ASCE)CF.1943-5509.0000281).
- Hulagabali, A.M., Solanki, C.H., Dodagoudar, G.R., and Shettar, M.P., 2018. Effect of reinforcement, backfill and surcharge on the performance of reinforced earth retaining wall, Asian Research Publishing Network (ARPN). *ARPN Journal of Engineering and Applied Sciences*, **13** (9): 3224-3230.
- Lai, Y.P., Bergado, D.T., Lorenzo, G., and Duangchan, T., 2006. Full scale reinforced embankment on deep jet mixing improved ground. *Ground Improvement Journal*, **10** (4): 153-164.
- Li, J., Tang, C., Wang, D., Pei, X., and Shi, B., 2014. Effect of discrete fiber-reinforcement on soil tensile strength. *Journal of Rock Mechanics and Geotechnical Engineering*, **6** (2): 133-137. <https://doi.org/10.1016/j.jrmge.2014.01.003>.
- Menil, N.J.L., 1993. Performance and interaction of Polymer grid based on laboratory test and a full scale test embankment. M. Eng. Thesis No. GT-93-10, Asian Institute of Technology, Bangkok, Thailand.
- Mitchell, K.J., and Villet, W.C.B., 1987. Reinforcement of earth slopes and embankments. NCHRP Report 290, Transportation Research Board, Washington D.C.: 182-184.
- Moudabel, O.A.M., Gregory, G.H., and Yang, X., 2014. Cross SA. A case study of MSE wall stability: comparison of limit equilibrium and numerical methods. *Ground Improvement and Geosynthetics*, GSP 238: 464-470. <https://doi.org/10.1061/9780784413401.046>.
- Nualkiang, M., 2011. Behavior of MSE wall/embankment with geogrid and metallic reinforcements on hard foundation. M. Eng. Thesis No. GT-10-05, Asian Institute of Technology, Bangkok, Thailand.
- Shivashankar, R., 1991. Behavior of mechanically stabilized earth (MSE) embankment with poor quality backfills on soft clay deposits, including a study of the pullout resistances. D.Eng Dissertation No. GT-90-03, Asian Institute of Technology, Bangkok, Thailand.
- Shrestha, S., Baral, P., Bergado, D.T., Chai, J.C., and Hino, T., 2014. Numerical simulation using FEM 2D and 3D compared with observed behavior of reinforced full scale embankment. *Proc. 9<sup>th</sup> International Symposium on Lowland Technology*, Saga University, Japan.
- Voottipruex, P., 2000. Interaction of hexagonal wire reinforcement with silty sand backfill soil and behavior of full scale embankment reinforced with hexagonal wire. D.Eng dissertation No. GT-99-01. Asian Institute of Technology, Bangkok, Thailand.
- Won, M.S., Langcuyan, C.P., Ann, S.J., and Lee, S.D., 2018. Behavior of MSE wall with strips and geogrids reinforcement subjected to compaction loadings, *IOSR Journal of Mechanical and Civil Engineering (IOSR-JMCE)*, **15** (2): 01-09.
- Yang, G.Q., Ding, J.X., and Zhouetal, Q.Y., 2010. Field behavior of a geogrid reinforced soil retaining wall with a wrap-around facing. *Geotechnical Testing Journal*, **33** (1): 1-6. <https://doi.org/10.1520/GTJ102410>.